

Impact of single string structure and multiple string interaction on strangeness production in Pb+Pb collisions at $\sqrt{s_{NN}} = 2.76$ TeV

Dai-Mei Zhou,^{1,*} Liang Zheng,^{2,†} Zhi-hong Song,¹ Yu-Liang Yan,³ Gang Chen,² Xiao-Mei Li,³ Xu Cai,¹ and Ben-Hao Sa^{3,1,‡}

¹*Key Laboratory of Quark and Lepton Physics (MOE) and
Institute of Particle Physics,
Central China Normal University,
Wuhan 430079, China*

²*School of Mathematics and Physics,
China University of Geosciences (Wuhan),
Wuhan 430074, China*

³*China Institute of Atomic Energy, P. O. Box 275 (18), Beijing 102413, China
(Dated: March 17, 2024)*

We present a systematic study on the strange and multi-strange particles production in Pb+Pb collisions at $\sqrt{s_{NN}} = 2.76$ TeV based on the PACIAE model simulations. Two different mechanisms, namely the single string structure variations and multiple string interactions, are implemented in the simulations. These modifications give rise to an enhancement of the string tension value involved in the Lund string fragmentation framework and generate more strange particles in the hadronic final state. By comparing the simulation results with the ALICE experimental data, it turns out that the inclusion of the variable effective string tension in the PACIAE model is capable to reach an improved agreement between theory and experiment on the strangeness production in Pb+Pb collisions.

I. INTRODUCTION

The study of strange and multi-strange particle production in relativistic heavy-ion collisions is an important tool to investigate the properties of the created strongly interacting QCD system, called Quark-Gluon Plasma (QGP). The enhancement of strangeness in heavy-ion collisions was one of the earliest proposed signals for QGP formation. For the hadronic scattering in vacuum, the strangeness content in the created particles is much smaller compared to the lighter components due to the mass suppression effect in the particle productions. The mass of the strange quark is close to the deconfinement temperature needed to create the QGP matter, allowing for the thermal production of strange quarks and also favoring the formation of multi-strange hadrons [1, 2]. As the lifetime of the QGP is estimated to be long enough for the full equilibration of strange quarks, a higher abundance of strangeness production per participant pair is expected in heavy-ion collisions than what is seen in proton-proton interactions. ALICE Collaboration reported a series of surprising strangeness enhancement observations in small collision systems like pp and pA [3–5]. They measured the yield ratios of multi-strange hadrons to charged pions as a function of multiplicity. These ratios are found to grow rapidly with multiplicity in pp collisions, and reach the values close to ones in PbPb collisions at full equilibrium in high multiplicity pPb collisions. It is interesting to notice that the

strangeness-to-pion ratios do not depend on the energy and size of collision system.

Different models are trying to interpret this universal strangeness-to-pion ratio as a function of the event multiplicity. The THERMUS statistical hadronization model suggest the suppression of strange hadron production in pp may come from the explicit conservation of strangeness quantum number based on the canonical approach [6, 7]. The EPOS model [8] assumes the QGP matter is partly formed in the pp collisions treating the interactions based on a core-corona approach. The DIPSY model [9] employs the color ropes mechanism [10, 11] taking into account the color interactions between overlapping strings and usually can reasonably describe the hierarchy of strangeness production. Other interesting extensions to the Lund string fragmentation model considering the thermodynamic features of strings in a dense environment [12] are implemented in PYTHIA8 [13] for data comparison as well. While various models can describe some key features of the data, the fundamental origin of enhanced strangeness production is still largely unknown. It suggests further developments are needed to reach a complete microscopic understanding of strangeness production in small systems and to identify whether such mechanisms would contribute to the observed effects in heavy-ion collisions.

In the Ref. [14], we introduced an effective string tension stemming from the single string structure and multiple string interaction to reduce the strange quark suppression in pp collisions based on the tunneling probability in Lund string fragmentation regime. These two mechanisms are implemented in the PACIAE Monte Carlo event generator [15] to study the strange hadron production in $\sqrt{s} = 7$ TeV pp collisions. We find that the

* zhoum@mail.ccnu.edu.cn

† zhengliang@cug.edu.cn

‡ sabh@ciae.ac.cn

inclusion of variable effective string tension yields an improved agreement between theory and experiment, especially for the recently observed multiplicity dependence of strangeness enhancement in pp collisions. This approach provides us a new method to understand the microscopic picture of the novel high multiplicity pp events collected at the LHC in the string fragmentation framework. In this work, we will extend this framework to describe heavy-ion collisions and study the strange and multi-strange particle productions in Pb+Pb collisions at $\sqrt{S_{NN}} = 2.76$ TeV.

II. MODEL SETUP

The PACIAE model is based on parton initial states generated by PYTHIA convoluted with the nuclear geometry implementing via the Glauber model [16]. The partonic rescattering is introduced after the creation of parton initial condition while the hadronic rescattering may happen after the hadronization of QCD matter. Thus, the PACIAE model can be employed to simulate a wide range of collision systems from nucleon-nucleon collision system to nuclear-nuclear collision system. We give more detailed information about PACIAE model in [15].

In this paper we extend the effective string tension approach to the description of nuclear-nuclear collisions by assuming the parametrization for single string structure is the same as that in pp collisions. Therefore the parameterized effective string tension responsible for the single string structure is given as:

$$\kappa_{eff}^s = \kappa_0(1 - \xi)^{-a}, \quad (1)$$

where κ_0 is the pure $q\bar{q}$ string tension usually set to 1 GeV/fm, a is a parameter to be tuned with experimental data while ξ can be parameterized as:

$$\xi = \frac{\ln(\frac{k_{\perp, max}^2}{s_0})}{\ln(\frac{s}{s_0}) + \sum_{j=gluon} \ln(\frac{k_{\perp, j}^2}{s_0})}, \quad (2)$$

with k_{\perp} being the transverse momentum of the gluons inside a dipole string. \sqrt{s} and $\sqrt{s_0}$ give the mass of the string system and a parameter related to the typical hadron mass, respectively. The quantity ξ quantifies the difference of a gluon wrinkled string compared to a pure $q\bar{q}$ string, assuming the fractal structure of a string object is dominated by the hardest gluon on the string. $(1 - \xi)^{-1}$ in Eq. 1 thus describes the multiplicity enhancement factor of the hardest gluon to the rest of the string component and can be related to the string tension with a scaling formula. The value of this string tension changes on a string-by-string basis in the current implementation and takes the string-wise fluctuations into consideration.

The multiple string interaction effects raised from the correlation of strings overlapped in a limited transverse

space are parameterized in a similar way of the close-packing strings [12] in pp collisions as follows:

$$\kappa_{eff}^m = \kappa_0(1 + \frac{n_{MPI} - 1}{1 + p_{T, ref}^2/p_0^2})^r, \quad (3)$$

In heavy ion collisions, the multiple string interaction effects will be stronger than pp collisions, due to the enhanced string density generated with multiple nucleon-nucleon collisions. Thus, we extend Eq. 3 to

$$\kappa_{eff}^m = \kappa_0(1 + \frac{N_{coll}}{N_{part}} \frac{n_{MPI} - 1}{1 + p_{T, ref}^2/p_0^2})^r, \quad (4)$$

in which n_{MPI} indicates the number of multiple parton interactions in one nucleon-nucleon collision. N_{coll} is the number of binary collisions and N_{part} is the number of participant nucleons in a nuclear-nuclear collision. Other parameters are chosen to be $p_{T, ref}^2/p_0^2 = 1$, $r = 0.2$, the same as in pp collisions [14].

Additionally, the string-wise single string structure and event-wise multiple string interaction effects can be combined together by replacing the κ_0 in Eq. 4 with κ_{eff}^s . Assuming $\kappa_0 = 1$ GeV/fm, one can derive a combined effective string tension as a product of the two:

$$\begin{aligned} \kappa_{eff}^{s+m} &= \kappa_{eff}^s (1 + \frac{N_{coll}}{N_{part}} \frac{n_{MPI} - 1}{1 + p_{T, ref}^2/p_0^2})^r \\ &= \kappa_{eff}^s \times \kappa_{eff}^m. \end{aligned} \quad (5)$$

The factor of N_{coll}/N_{part} introduced in Eq.(5) amplifies the multiple string interaction effects and delivers the variational string tension at high multiplicity for nuclear-nuclear collisions. Figure. 1 shows the ratio of N_{coll} to N_{part} varying with collision centrality from the PACIAE calculations. This term accounts for the major system size dependence effect in our effective string tension approach.

In the Lund string fragmentation regime, the following parameters are expected to evolve according to the change of the effective string tension:

- PARJ(1) is the suppression of diquark-antidiquark pair production compared to the quark-antiquark production,
- PARJ(2) is the suppression of s quark pair production compared to the u or d pair production,
- PARJ(3) is the extra suppression of strange diquark production compared to the normal suppression of strange quark,
- PARJ(21) (denoted by σ) corresponds to the width σ in the Gaussian p_x and p_y transverse momentum distributions for primary hadrons.

These Lund string fragmentation parameters can be related to the effective string tension through a scaling function implied by the tunneling probability:

$$\lambda_2 = \lambda_1^{\frac{\kappa_{eff}}{\kappa_2^2}}, \quad (6)$$

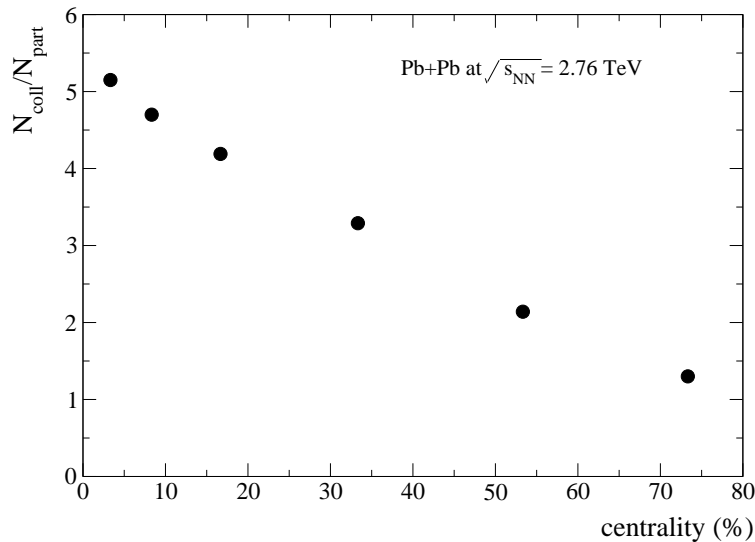


FIG. 1. $N_{\text{coll}}/N_{\text{part}}$ varying with the collision centrality

where λ refers to PARJ(1) or PARJ(2) or PARJ(3) etc. In the above equation, κ_1^{eff} represents the string tension in vacuum (usually assigned with $\kappa_1^{\text{eff}}=1$ GeV/fm) and λ_1 shows the corresponding fragmentation parameter values. κ_2^{eff} gives the effective string tension taking into account the string tension variation impacts. The fragmentation parameter λ_2 will be enlarged when the effective string tension κ_2^{eff} becomes greater than κ_1^{eff} . Similarly, the fragmentation p_T width PARJ(21) varies with the effective string tension as

$$\sigma_2 = \sigma_1 \left(\frac{\kappa_2^{\text{eff}}}{\kappa_1^{\text{eff}}} \right)^{1/2}. \quad (7)$$

In the rest of the work, we will focus on the comparison of our PACIAE calculations to the ALICE PbPb 2.76 TeV data and study the variational string tension effects on the centrality dependence of strange hadron productions. In order to describe the mid-rapidity charged particle yields $\frac{dN_i}{dy}|_{|y|<0.5}$ of ALICE experimental results [25] by PACIAE model, three parameters are tuned PARP(31)=2.7(K factor) for the hard scattering cross sections, PARJ(41)=1.7(α) and PARJ(42)=0.09(β) in the LUND string fragmentation function. PACIAE model gives mid-rapidity particle yields $\frac{dN_i}{dy}|_{|y|<0.5}$ for $\pi^+ = 722.5$ and $\pi^- = 722.2$ for 0 – 5% centrality case, consistent with the corresponding ALICE data $\pi^+ = 733 \pm 54$ and $\pi^- = 732 \pm 52$. These parameters were fixed for the simulation of other event centralities. The other fragmentation parameters modified by the effective string tension are determined with the reference values PARJ(1)=0.1, PARJ(2)=0.3, PARJ(3)=0.4 and PARJ(21)=0.85 in the vacuum.

III. RESULTS

To investigate the influence of different effective string tensions, on the strangeness production in PbPb collisions at $\sqrt{s_{NN}} = 2.76$ TeV, we first perform an examination on the mean participant number dependence of the charged pion and proton yields in Fig. 2. Model predictions with the default string tension κ_0 , single string structure κ_{eff}^s , multiple string interactions κ_{eff}^m , the combination of $\kappa_{\text{eff}}^{s+m}$, and the $\kappa_{\text{eff}}^{s+m(*)}$ with 1.5 times enlarged default parameters of PARJ(2) and PARJ(3) are shown as the solid, dashed, dash-dot-dotted, dash-dotted, and the dotted curves, respectively. ALICE data are indicated by the red markers [25]. The results indicate scenarios with larger string tension, in which strings become more difficult to break up, generally produce less pions and protons. The impacts on pion or proton multiplicity can be as large as 30% varying from κ_0 to $\kappa_{\text{eff}}^{s+m}$.

In Fig. 3, we show a comparison of the simulation results for particles with different strangeness number dependent on $\langle N_{\text{part}} \rangle$ to ALICE data. All the strange particle productions are found to be enhanced with the inclusion of increased effective string tension. As can be seen in Fig. 3(a), K_S^0 calculation with κ_0 is consistent with data in peripheral collisions, while larger effective string tension is needed especially for the most central collisions, comparing with the ALICE measurement [26]. The impact of effective string tension on the strange baryon production is much more pronounced than that on K_S^0 . In the strange baryon comparisons, the slope change due to effective string tension shows a clear hierarchy depending on the strangeness number. The change of the slope from the minimum effective string tension (κ_0) to the maximum one ($\kappa_{\text{eff}}^{s+m(*)}$) in Λ production is the smallest, while the Ω slope changes most dramatically from κ_0 to

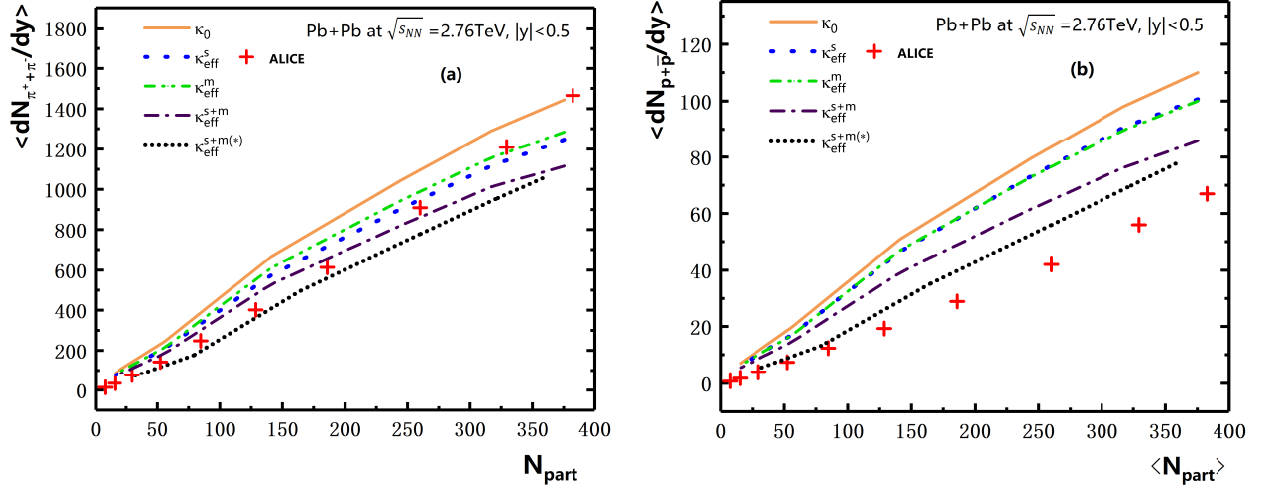


FIG. 2. (Color online) Pion (a) and proton (b) midrapidity particle yields $\frac{dN_i}{dy}|_{|y|<0.5}$ varying with $\langle N_{part} \rangle$ in PbPb collisions at $\sqrt{s_{NN}} = 2.76$ TeV for different string environments: constant string tension (κ_0 , solid line), single string structure (κ_{eff}^s , dashed line), multiple string interaction (κ_{eff}^m , dash-dot-dotted line), single+multiple string environment (κ_{eff}^{s+m} , dash-dotted line), as well as the single+multiple with a zero approximation of PARJ(2) and PARJ(3) enlarged to 1.5 times of the corresponding default values ($\kappa_{eff}^{s+m(*)}$, dotted line). The experimental data are denoted as crosses and taken from [25].

$\kappa_{eff}^{s+m(*)}$ environments. The multiple string interaction (κ_{eff}^m) seems to be important to fit the Λ result in these comparisons [26]. The Ξ result [27] can be described reasonably with the calculation based on the κ_{eff}^{s+m} assumption. However, for Ω productions [27], one will need to increase the reference values of PARJ(2) and PARJ(3) by a factor of 1.5 to describe the data when both single string structure variation and multiple string interaction effects on ($\kappa_{eff}^{s+m(*)}$).

Aside from examining the integrated yield of particles as a function of the $\langle N_{part} \rangle$, it is also of great interest to understand the relative production of strange particles. Figure. 4 shows strange particle relative to π production for K_S^0 , Λ , Ξ and Ω . It is obvious to see these ratios strongly depend on the choice of the string tension assumptions. For the situation with large effective string tension, the strange to pion ratios are significantly enhanced. The magnitude of enhancement is related to the strangeness number. The factor of enhancement is found to be larger for the multi-strange baryons. On the other hand, it is also a bit surprising to see the strange to pion ratios are almost independent of the $\langle N_{part} \rangle$ in each case. This behavior can be understood with the scaling feature of our two string tension variation mechanism. For the single string structure, it is mostly energy dependent and has no strong correlation with the $\langle N_{part} \rangle$. For the multiple string interaction, the effective string tension changes rather slowly with N_{part} as r is 0.2 in Eq. 4 leading to a mild growth on the system size. By combining these two effects, the magnitude of effective string tension may change significantly with different string tension assumptions, but does not rely on the event centrality. The weak N_{part} dependence of multi-strange to pion ratios in the

heavy ion collision system provided by these model implementations are qualitatively confirmed by the ALICE data. This comparison implies the effective string tension approach can be an essential phenomenological tool to understand the origin of strangeness enhancement effect.

IV. DISCUSSIONS AND CONCLUSIONS

We provide a systematic study on the strange particle productions in high energy PbPb collisions based on the variational effective string tension approach in PACIAE. In the comparison of integrated particle yields, the effects of string tension variations are found to be important to describe the $\langle N_{part} \rangle$ dependence especially for the multi-strange hadrons. The slope change due to effective string tension shows a clear hierarchy depending on the strangeness number.

The strange particles relative to π production are studied as well. PACIAE model simulations elucidate that for different string tensions, the ratios are generally larger with stronger effective string tension. However, for each string tension assumption, the strange to pion ratios are rather flat across different event centralities, which is consistent with the observations in the ALICE data. Our findings in this work suggest the effective string tension approach implemented in PACIAE can provide the qualitative feature of the enhanced strange particle production, which has been considered to be a defining signal for QGP creation in heavy ion collisions for a long time. The implementation of this framework in PACIAE will pave the way for a new perspective to understand the

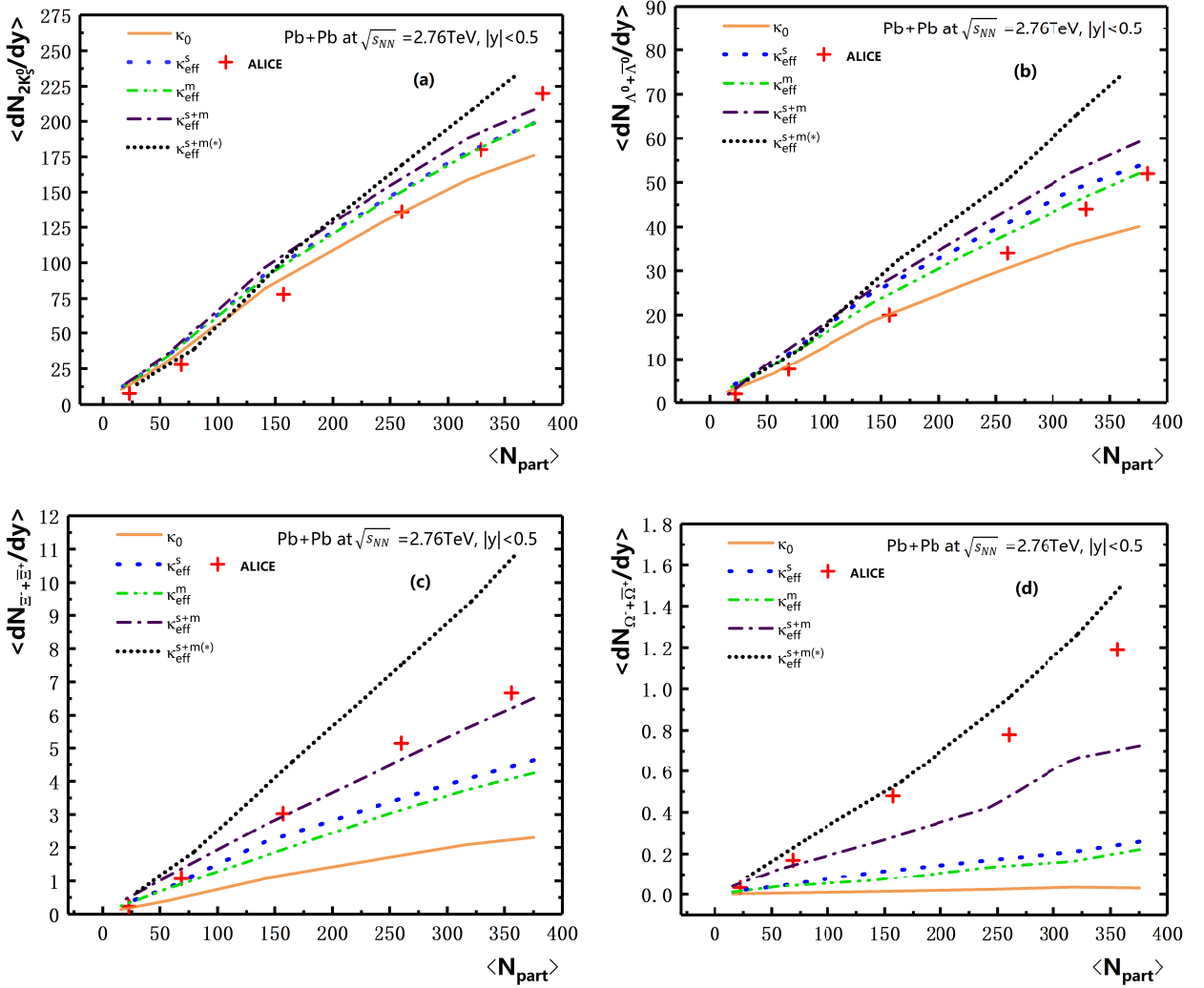


FIG. 3. (Color online) Integrated strange and multi-strange mid-rapidity yields, dN/dy , varying with the $\langle N_{part} \rangle$ in the PbPb collisions at $\sqrt{s_{NN}} = 2.76$ TeV: K_S^0 (a), Λ (b), Ξ (c) and Ω (d). Five different string environments are shown: κ_0 , solid curve; κ_{eff}^s , dashed curve; κ_{eff}^m , dash-dot-dotted curve; κ_{eff}^{s+m} , dash-dotted line; and $\kappa_{eff}^{s+m(*)}$, dotted curve. The experimental data for K_S^0 and Λ are taken from [26], for Ξ and Ω are taken from [27].

strangeness enhancement effect observed in nuclear collisions.

ACKNOWLEDGMENTS

This work was supported by the National Natural Science Foundation of China (11775094, 11905188, 11775313), the Continuous Basic Scientific Research Project (No.WDJC-2019-16), National Key Research and Development Project (2018YFE0104800) and by the 111 project of the foreign expert bureau of China.

[1] J. Rafelski, B. Müller, Phys. Rev. Lett. 48, 1006 (1982).
 [2] P. Koch, J. Rafelski, W. Greiner, Phys. Lett. B 123, 151 (1983).
 [3] J. Adam et al. (ALICE): Nature Phys., 13, 535 (2017).
 [4] S. Acharya et al. (ALICE), Eur. Phys. J. C **80**, 167

(2020).
 [5] J. Adam et al. (ALICE), Phys. Lett. B **758**, 389 (2016).
 [6] V. Viskovic and A. Kalweit, arXiv:1610.03001.
 [7] ALICE Collaboration, Phys. Rev. C 99, 024906 (2019).
 [8] T. Pierog, I. Karpenko, J. M. Katzy, E. Yatsenko, and

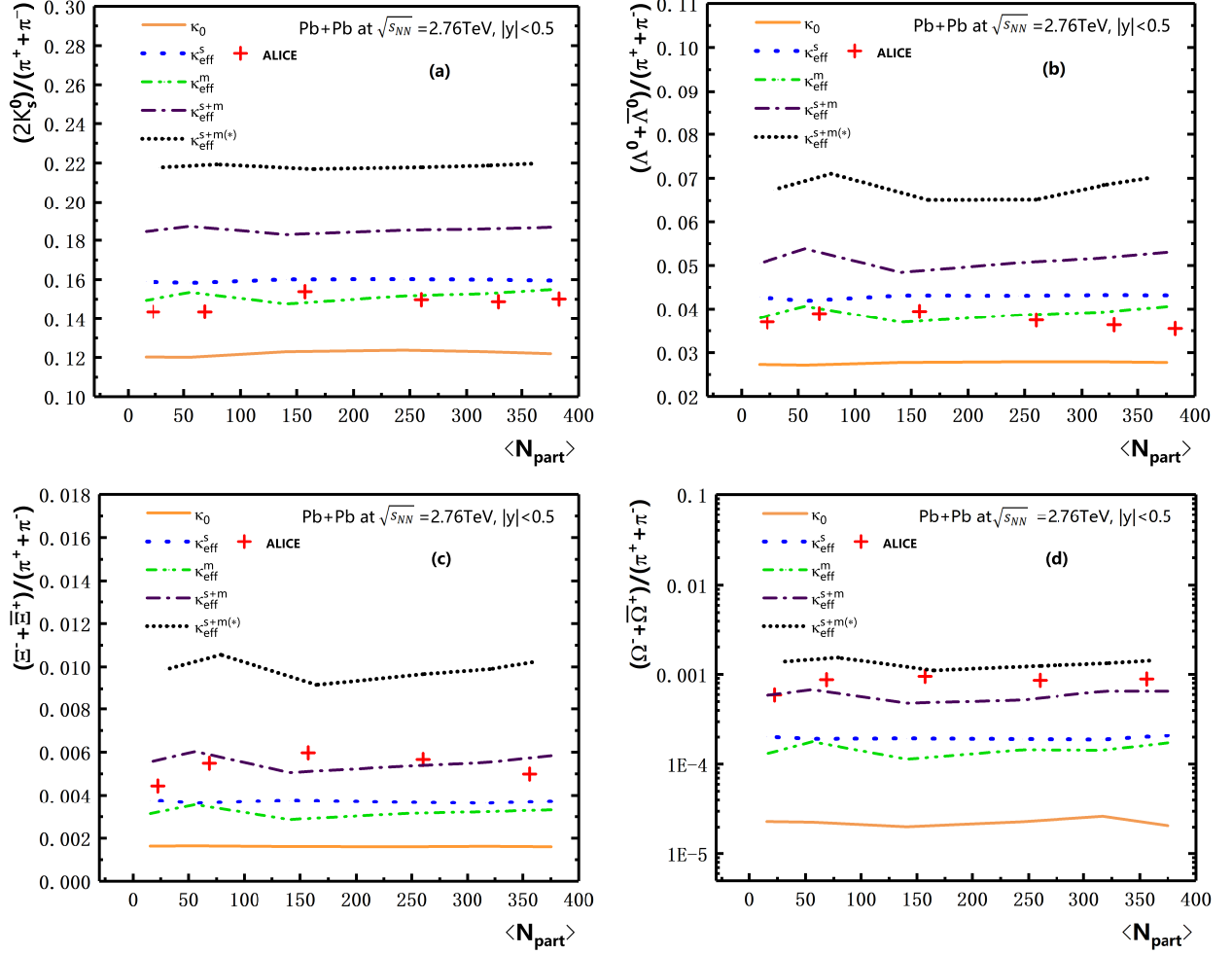


FIG. 4. (Color online) Ratio of strange and multi-strange particles to pion varying with the $\langle N_{part} \rangle$ in Pb+Pb collisions at $\sqrt{s_{NN}} = 2.76$ TeV. Five different string environment are shown: κ_0 , solid curve; κ_{eff}^s , dashed curve; κ_{eff}^m , dash-dot-dotted curve; κ_{eff}^{s+m} , dash-dotted curve; and $\kappa_{eff}^{s+m(*)}$, dotted curve. The ALICE data are denoted as crosses and taken from [25–27]

- K. Werner, Phys. Rev. C 92, 034906 (2015).
- [9] C. Bierlich, G. Gustafson, L. Lönnblad, A. Tarasov, J. High Energy Phys. 03 (2015) 148.
- [10] T. S. Biro, H. B. Nielsen, and J. Knoll, Nucl. Phys. B 245, 449 (1984).
- [11] B. Andersson and P.A.Henning, Nucl. Phys. B 355, 82 (1991).
- [12] N. Fischer and T. Sjöstrand, J. High Energy Phys. 01 (2017) 140.
- [13] T. Sjöstrand, S. Ask, J. R. Christiansen, R. Corke, N.Desai, P. Ilten, S. Mrenna, S. Prestel, C. O. Rasmussen, and P.Z. Skands, Comput. Phys. Commun. 191, 159 (2015).
- [14] Liang Zheng, Dai-Mei Zhou, Zhong-Bao Yin, Yu-Liang Yan, Gang Chen, Xu Cai, and Ben-Hao Sa, Phys. Rev. C 98, 034917 (2018).
- [15] Ben-Hao Sa, Dai-Mei Zhou, Yu-Liang Yan, Xiao-Mei Li, Shene-Qin Feng, Bao-Guo Dong, and Xu Cai., Comput. Phys. Commun. 183, 333 (2012); *ibid*, 224, 412 (2018).
- [16] T. Sjöstrand, S. Mrenna, and P. Skands, J. High Energy Phys. 05, 026 (2006).
- [17] A. Tai and B.H.Sa, Phys. Lett. B 409, 393 (1997).
- [18] A. Shor and R. Longacre, Phys. Lett. B 218, 100 (1989).
- [19] B. I. Abelev, et al., STAR Collaboration, Phys. Rev. C 79, 034909 (2009).
- [20] B. I. Abelev, et al., ALICE Collaboration, Phys. Rev. C 88, 044909 (2013).
- [21] D. Miskowiec, <http://www.linux.gsi.de/~misko/overlap/>.
- [22] B. L. Combridge, J. Kripfgang, and J. Ranft, Phys. Lett. B 70, 234 (1977).
- [23] R. D. Field, Application of perturbative QCD, Addison-Wesley Publishing Company, Inc., 1989.
- [24] P. Z. Skands, Phys. Rev. D 82, 074018 (2010)
- [25] B. Abelev et al., (ALICE Collaboration), Phys. Rev. C 88, 044910 (2013)
- [26] ALICE Collaboration, Phys. Rev. Lett. 111, 222301 (2013)
- [27] ALICE Collaboration, Phys. Lett. B 728, 216-227 (2014)